JOC The Journal of Organic Chemistry

Article

pubs.acs.org/joc

Singlet vs Triplet Reactivity of Photogenerated α,n-Didehydrotoluenes

Chiara Pedroli, Davide Ravelli,* Stefano Protti, Angelo Albini, and Maurizio Fagnoni*

Department of Chemistry, PhotoGreen Lab, Viale Taramelli 12, 27100 Pavia, Italy

Supporting Information

ABSTRACT: The reactivity of α,n-didehydrotoluenes (DHTs) in protic media (organic/aqueous mixtures) was explored by means of a combined computational and experimental approach. These intermediates were generated via a photoinduced double elimination process occurring in (chlorobenzyl)trimethylsilanes and led to the formation of a varied products distribution, depending on the isomer tested. Irradiation of ortho- and para-derivatives resulted, respectively, in the formation of triplet α,2- and α,4-DHTs, whose diradical reactivity led to both radical and polar products. On the other hand, irradiation of the meta-precursor led to the singlet α,3-DHT isomer. The latter showed a marked preference for the formation of polar products and this was rationalized, as supported by computational evidence, via the involvement of a zwitterionic species arising through interaction of the nucleophilic solvent with the benzylic position of the DHT.

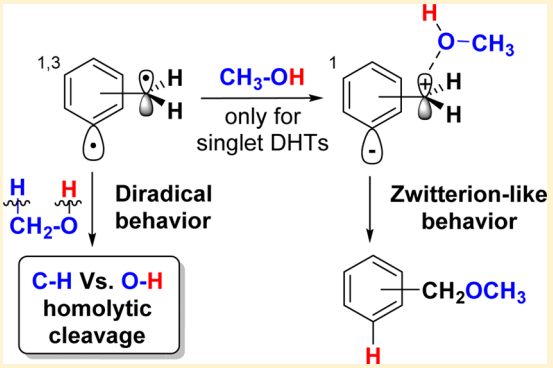

INTRODUCTION

In organic molecules the covalent bond, that is the sharing of two (or more) electrons between two atoms, is what typically makes molecules stable. Chemical reactions most often occur by cleaving a bond and thus via high energy intermediates (a couple of radicals or a couple of ions),[1] unless the simultaneous formation of another bond leads back to stability (as typical of concerted processes).[2] When the fragments are bonded, diradicals[3] or zwitterions are formed (Scheme 1a).[4]

Scheme 1. (a) Generation of a Biradical and a Zwitterion via Homolytic and Heterolytic Bond Cleavage and (b) Bergman Cycloaromatization of Enediynes for the Generation of 1,4-Benzynes

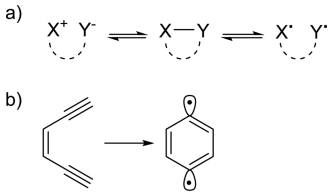

The competition between homo- and heterolytic cleavage of a bond is thus a phenomenon of general interest.[1,5] The observed reactivity, viz. atom abstraction or cation (anion) transfer, is the election tool to have insight on the lysis mechanism and enables a better characterization of the intermediates. An intriguing case is that of cycloaromatizations, such as the Bergman reaction,[6,7] where a new σ bond is formed at the expenses of two π bonds. As a result, a *p*-benzyne intermediate is generated, endowed with a peculiar dual reactivity, showing either a diradical[1,5,8,9] or a zwitterionic[10] behavior (Scheme 1b). A related case is represented by didehydrotoluenes (DHTs, **II**; Scheme 2), intermediates formally resulting from the elimination of two hydrogen

Scheme 2. Generation of α,n-DHTs via (a) Myers-Saito Cycloaromatization of Enyne-Allene I and (b) Photolysis of Benzyl Derivatives V

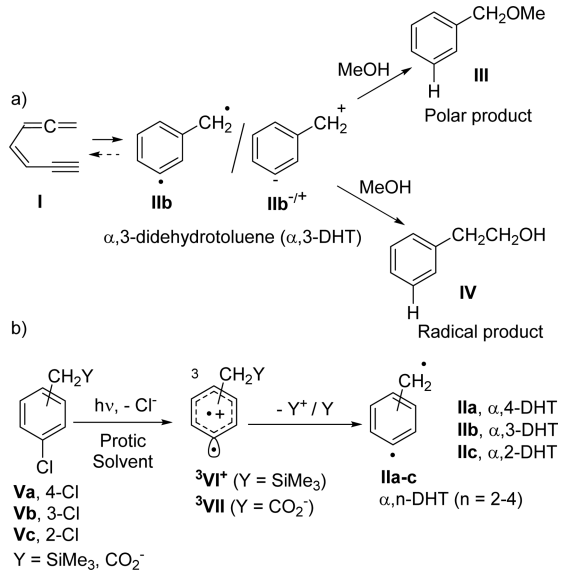

Received: March 14, 2017
Published: June 7, 2017

DOI: 10.1021/acs.joc.7b00610
J. Org. Chem. 2017, 82, 6592−6603

atoms from a toluene molecule, one from the benzylic position and one from the ring. Accordingly, these are heterosymmetric species ($\sigma^1\pi^1$), where the two centers are not expected to interact due to geometric factors. Depending on the relative arrangement of the two radical centers, three isomeric DHTs, namely α,4- (**IIa**), α,3- (**IIb**), or α,2-DHT (**IIc**), are possible and all of them can exist in two different spin states, either the singlet or the triplet. Theoretical investigations demonstrated that the α,4- and α,2-DHTs are ground state triplets (with a triplet-singlet gap of 7.4 and 8.1 kcal mol^{-1}, respectively), while in the case of the α,3-isomer the two states are closer in energy, with the singlet slightly more stable than the triplet (3.0 kcal mol^{-1} gap).[11,12]

Notably, intermediates containing the α,3-DHT moiety are known to have a cytostatic activity, that has been attributed to their capability of cleaving DNA.[13] In fact, highly unsaturated hydrocarbons, such as enyne-allenes (**I**, Scheme 2a), present in natural (as an example, the properties of antibiotic Neocarzinostatin are due to its conversion to an activated derivative containing the enyne-allene moiety)[14,15] or artificial[9,16,17] compounds, may cyclize via diradical intermediates. A typical case is the Myers-Saito reaction, where α,3-didehydrotoluenes are exclusively formed.[14,18] Indeed, model studies have revealed the formation of products expected from both radical and ionic paths.[1] As a matter of fact, α,3-didehydrotoluenes can lead (among others) to both benzyl methyl ether (**III**) and phenethyl alcohol (**IV**) in the reaction with MeOH in variable amounts.[1,19] This calls for a diradical/zwitterion dichotomy for α,3-DHTs (see structures **IIb**/**IIb**$^{-/+}$) where, however, in both cases either a hydrogen atom or a proton transfer from the medium to **IIb** or **IIb**$^{-/+}$ is the first step involved.[18d]

While the formation of radical products can be easily explained by considering the diradical nature of α,3-DHT, more difficult is the rationalization of polar products formation. Originally, it was proposed that O−H insertion products could be explained on the basis of a resonance between diradical **IIb** and zwitterion **IIb**$^{-/+}$, sharing a negative charge at the dicoordinated carbon and a positive one at the benzylic position.[18d] Such resonance, however, is symmetry forbidden and the zwitterion is actually an excited state of **IIb**.[20] Indeed, experimental studies ruled out the likelihood of a single intermediate mechanism, where the diradical and the zwitterion are in resonance.[20,21] Nevertheless, a recent report supported that a part of the Myers-Saito reaction follows a nonadiabatic course. Thus, the zwitterion was predicted to form directly from the enyne-allene, in a postrate-determining bifurcation. A post-transition state nonadiabatic transition from the ground-state singlet of enyne-allene to the excited-state singlet zwitterion was then invoked.[22]

Such scenario, however, applies only to the Myers-Saito reaction and to the reactivity of α,3-DHT, the only isomer accessible by this approach. In view of this, we reconsidered our recently developed alternative access to all α,*n*-DHTs, including thermally inaccessible **IIa** and **IIc** isomers. This involves a one-photon, double elimination of a nucleofugal group (chloride,[19,23,24] sulfonate,[25] or phosphate[25] anions) and an electrofugal moiety (trimethylsilyl cation[19,23,25] or carbon dioxide[24]) from aromatic compounds (**Va-c**), occurring efficiently at room temperature via triplet phenyl cations (^{3}**VI**$^+$ or ^{3}**VII**, respectively; Scheme 2b). Interestingly, the products distribution observed when generating **IIb** under thermal conditions from enyne-allene **I** and under irradiation conditions from (3-chlorobenzyl)trimethylsilane is roughly the same.[19]

It appeared worthwhile to unravel the nature of the involved intermediates by generating the three isomeric α,*n*-DHTs and analyzing the distribution of the products obtained depending on the reaction conditions. This investigation should help in the rationalization of the diradical/zwitterion dichotomy observed in α,*n*-DHTs chemistry, being thus beneficial in the comprehension of the mode of interaction of didehydrotoluenes with the surrounding medium in biological systems. We thus investigated the photochemistry of the three isomeric (chlorobenzyl)trimethylsilanes **1a−c** in protic media and in the presence of suitable additives (Schemes 3−7). The rationalization of the reactivity offered was supplemented also by computational analysis. The results of this study are reported below.

Scheme 3. Photoreactivity of Chlorobenzylsilanes 1a−c in MeOH/H_2O 4:1 Mixture

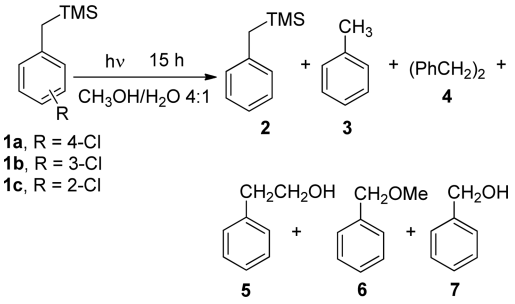

RESULTS

As mentioned in the Introduction Section, the photochemical decomposition of **1a−c** in protic solvents involves a heterolytic dechlorination and ensuing desilylation from the benzylic position.[19,23a] The study was carried out in organic/aqueous mixtures, maintaining the highest amount of water possible (solvent/H_2O ratio from 4/1 to 2/1) for dissolving **1a−c** (0.025 M). This choice was based on two grounds, viz. (i) in view of the closeness to biologic conditions, and (ii) because previous studies showed that dechlorination was efficient in the presence of water.[19,23,24] The irradiation was carried out for 15 h by using phosphor-coated lamps centered at 310 nm. The products formed are gathered in Table 1, where they have been divided in two classes, namely those assigned to the phenyl cation reactivity (dechlorinated/silylated products) and those deriving from α,*n*-DHTs (dechlorinated/desilylated products). The ratio between cation vs α,*n*-DHT deriving products and, in the latter case, the ratio between radical vs polar products have been likewise reported (see further the Discussion Section and Table S1 in the Supporting Information).

Irradiation in aqueous alcohols (MeOH, EtOH, *i*PrOH, *t*BuOH) yielded both silicon-containing products (benzylsilane **2**, phenols **8a−c**, as well as aromatic ethers **11a−c**, **13a−c**) and silicon-free compounds, viz. toluene **3**, bibenzyl **4**, α- (or β- in the case of *t*BuOH) benzylated alcohols **5**, **9**, **12** and **14**, as well as benzyl alcohol **7** and benzyl ethers **6**, **10**, and **15** (see Table 1 and Schemes 3 and 4).

The quantum yield of decomposition (Φ_{-1}) was particularly high in MeOH/H_2O 4/1, but reasonable values were found also in the other cases, the *t*BuOH/H_2O 3/1 mixture being the medium where compounds **1a−c** were less photoreactive. As for products distribution, dechlorinated **2** was formed in significant yields (20−49%) for **1b,c** in all of the solvents

DOI: 10.1021/acs.joc.7b00610
J. Org. Chem. 2017, 82, 6592−6603

Table 1. Irradiation of Compounds 1a−c in (Deuterated) Aqueous Alcohols[a]

halide	Φ_{-1}[b]	products (yield %)[c] cation products	products (yield %)[c] α,n-DHT products	cation/DHT[d]	radical/polar[e]
			CH_3OH/H_2O 4/1		
1a	0.73[f]	**2**, 3	**3**, 1; **4**, 23; **5**, 56; **6**, 5	3/97	94/6
1b	0.82[f]	**2**, 25	**5**, 12; **6**, 42; 7, 14	27/73	18/82
1c	0.27[f]	**2**, 49	**4**, 5; **5**, 23; **6**, 3	61/39	90/10
			$EtOH/H_2O$ 2/1		
1a	0.55	2, 2	3, 4; 4, 29; **9**, 59; **10**, 2	2/98	98/2
1b	0.28	2, 25; **8b**, 4	**3**, 1; **4**, 5; 7, 18; **9**, 32; **10**, 14	29/71	54/46
1c	0.41	**2**, 35; **8c**, 1	**3**, 3; **9**, 31	52/48	100/0
			$iPrOH/H_2O$ 4/1		
1a	0.20	2, 4	**3**, 12; **4**, 7; **12**, 56	5/95	100/0
1b	0.32	2, 37; **11b**, 6	**3**, 11; **12**, 27	53/47	100/0
1c	0.28	2, 45; **11c**, 3	**3**, 6; **12**, 22	63/37	100/0
			$tBuOH/H_2O$ 3/1		
1a	0.08		**4**, 9; 7, 5; **14**, 16; **15**, 10	0/100	62/38
1b	0.16	2, 21; **8b**, 10; **13b**, 8	**14**, 16; 7, 18; **15**, 13	45/55	34/66
1c	0.19	2, 20; **8c**, 3	7, 3; **14**, 12; **15**, 8	50/50	53/47
			CH_3OD/D_2O 4/1		
1a		2, 1	**4**, 23; **5**-d_1, 67; **6**-d_1, 3	1/99	97/3
1b		2, 31	**4**, 3; 5- d_1, 12; **6**-d_1, 22; 7-d_2, 7	41/59	34/66
1c		2, 40	**4**, 6; 5-d_1, 38; **6**-d_1, 3	46/54	94/6
			CD_3OH/H_2O 4/1		
1a			**4**-d_2, 14; **5**-d_3, 22; **6**-d_3, 11	0/100	77/23
1b		2-d_1, 23	**6**-d_3, 39; 7, 9	32/68	0/100
1c		2-d_1, 26	**4**-d_2, 6; 5-d_3, 22; **6**-d_3, 9	41/59	76/24

[a]Conditions: 0.025 M solution of **1a−c** in the chosen solvent irradiated at 310 nm. t_{irr} = 15 h (see also Table S1 in Supporting Information). [b]Quantum yields of disappearance (Φ_{-1}) of **1a−c** (10^{-2} M in the chosen media) were measured at 254 nm. [c]Yields were based on consumed **1a−c** and determined by GC analysis. [d]Ratio between phenyl cation vs DHT deriving products. [e]Ratio between radical vs polar α,n-DHTs deriving products. [f]From ref 19.

Scheme 4. Photoreactivity of 1a−c in Aqueous Alcohols

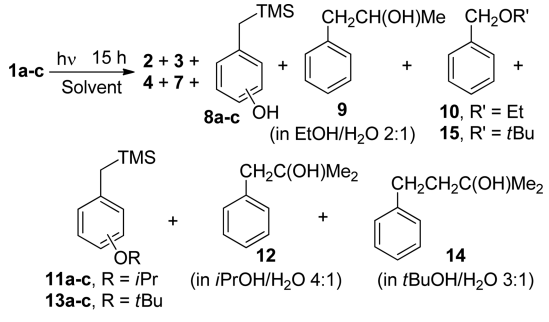

tested. Radical products (**3**−**5**, **9**, **12**, **14**) were predominant in the case of *para*- and *ortho*-chlorides **1a**,**c**.

By contrast, compounds arising from the polar pathway of DHTs were mainly formed in high yields in the case of **1b**. On the other hand, no polar product was obtained when using isopropanol/water as medium, independently from the considered isomer, whereas a competition between the two pathways took place in aqueous *tert*-butanol.

The reaction was then extended to deuterated methanol/water mixtures. Comparison with the non deuterated medium evidenced that shifting to CH_3OD/D_2O (Scheme 5a) halved

Scheme 5. Photoreactivity of 1a−c in (a) CH_3OD/D_2O 4:1 Mixture and (b) CD_3OH/H_2O 4:1 Mixture

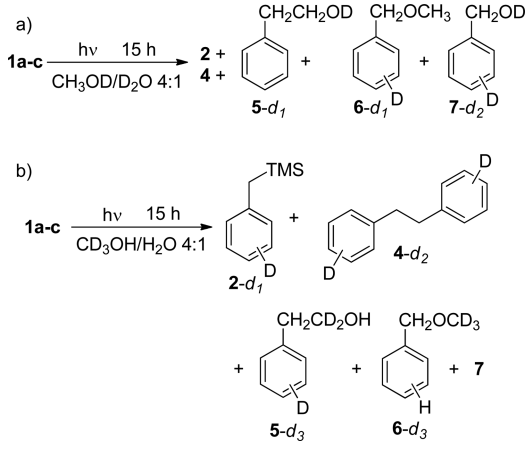

DOI: 10.1021/acs.joc.7b00610
J. Org. Chem. 2017, 82, 6592−6603

the yield of products **6** and **7** (in the case of **1a,b**), but had only a small effect on the other products yield. On the other hand, using the CD_3OH/H_2O mixture (Scheme 5b) diminished the yield of products **4** and **5** from **1a**, and of products **5** and **7** from **1b** (see Table 1, lower part).

In THF and 1,4-dioxane (2:1 with water), bibenzyl **4** and benzylated ethers **16** and **17** were the main products from the *para*-isomer (Table 2). Ether **17** was also formed in significant

Table 2. Irradiation of 1a−c in Aqueous Ethers and Acetonitrile[a]

		products (yield %)[c]			
halide	conv. (%)[b]	cation products	α,n-DHT products	cation/DHT[d]	radical/polar[e]
		THF/H_2O 2/1			
1a	73	**2**, 10	**4**, 11; **16**, 61	12/88	100/0
1b	55	**2**, 43	**16**, 1	98/2	100/0
1c	43	**2**, 33	**16**, 1	97/3	100/0
		dioxane/H_2O 2/1			
1a	100	**2**, 4	**4**, 10; **17**, 66	5/95	100/0
1b	100	**2**, 41	**4**, 3; **17**, 51	43/57	100/0
1c	100	**2**, 49	**17**, 32	61/39	100/0
		CH_3CN/H_2O 4/1			
1a	100		**4**, 15; **18**, 51	0/100	100/0
1b	19	**2**, 37		100/0	
1c	19	**2**, 23	**4**, 15	61/39	100/0

[a]See Table 1. [b]Conv. (%) = **1a−c** consumption (%). [c−e]See Table 1.

amounts from both the *ortho*- and *meta*-derivatives (Scheme 6). Nitrile **18** was formed instead in aqueous acetonitrile (4:1) only from **1a** and no solvent incorporating products were detected in the case of **1b** and **1c** (Scheme 6).

Scheme 6. Photoreactivity of 1a−c in Aqueous Dioxane, Acetonitrile, and THF

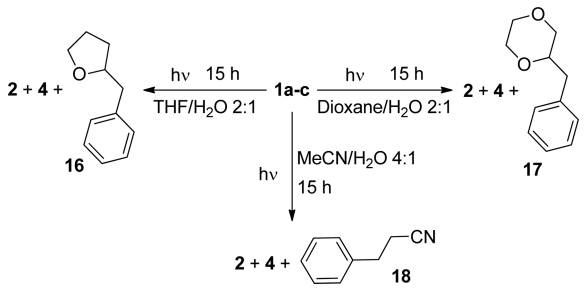

The reaction was then studied in MeOH/water 4:1 in the presence of some additives (Scheme 7). Thus, when 1,4-cyclohexadiene (CHD, 0.2 M) was present, toluene **3**, bibenzyl **4** (in the case of **1a**), benzylcyclohexadiene **19**, and benzyl methyl ether **6** (in the case of **1b**), as well as benzylsilane **2**, were formed in largely different yields from the three isomers (Table 3). CCl_4 (0.5 M) caused a lowering of the yield of **2**, while the main products were (2,2,2-trichloroethyl)benzene **20** (that is present only for isomers **1a,c**) and the three isomeric 1-chloro-*n*-(2,2,2-trichloroethyl)benzenes **21a−c** along with some ether **6** (only from the *meta*- isomer).

CALCULATIONS

To rationalize the reactivity observed for the three isomeric α,*n*-DHTs in different media, we undertook a computational

Scheme 7. Photoreactivity of 1a−c in the Presence of 1,4-Cyclohexadiene and CCl_4

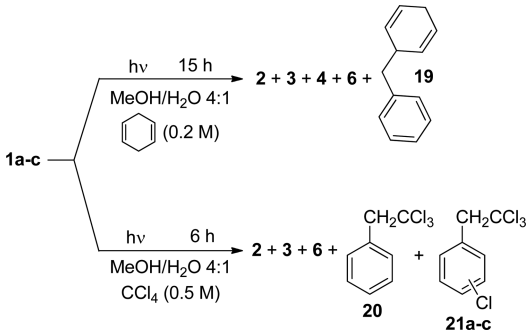

Table 3. Irradiations of 1a−c in MeOH/H_2O 4/1 in the Presence of Additives[a]

		products (yield %)[c]			
halide	conv. (%)[b]	cation products	α,n-DHT products	cation/DHT[d]	radical/polar[e]
		0.2 M 1,4-cyclohexadiene			
1a	99	2, 7	**3**, 40; **4**, 21; **19**, 31	7/93	100/0
1b	53	2, 75	3, 6; **6**, 11; **19**, 5	77/23	50/50
1c	61	2, 53	3, 3; 19, 3	89/11	100/0
		0.5 M CCl_4			
1a	56		**20**, 20; **21a**, 33	0/100	100/0
1b	8	2, 5	**6**, 21; **21b**, 72	5/95	77/23
1c	32	2, 11	**20**, 15; **21c**, 22	23/77	100/0

[a]See Table 1. [b]Conv. (%) = **1a−c** consumption (%). [c−e]See Table 1.

investigation to document the details of the reaction path describing the transfer of a hydrogen from the chosen solvent to DHTs. According to previous work by our group,[23] the theoretical method adopted here made use of a multiconfigurational approach, viz. the complete active space self-consistent field (CASSCF) method, required to correctly handle the peculiar electronic structure of DHTs, also including proper corrections to account for the solvent effect (an implicit model has been used) and for the dynamic electron correlation term (see Computational Methods for details). Furthermore, we also evaluated the role of specific interactions of DHTs with the medium by explicitly including solvent molecules into the simulation.

At the beginning, we focused our attention on the simplest system possible, viz. that involving the DHT and one molecule of solvent (MeOH). In particular, we optimized the transition states (TSs) describing the transfer of H from MeOH to the dicoordinated carbon of **IIa-c**, the most reactive site of the intermediate.[26] Two different kinds of transfer path have been considered, since the H atom may be abstracted from either the C−H or the O−H positions. As apparent from the structures of ^{3}**IIa** (taken as a model) reported in Figure 1, the methanol molecule assumes two different arrangements depending on the process considered, with the C_M−O bond lying slightly tilted or perpendicularly with respect to the ring of the DHT in the TS structures describing the C−H and the O−H transfer, respectively.

After optimization of the TSs, we investigated the corresponding intrinsic reaction coordinates (IRCs) in both directions to have an idea of the energy changes involved in the

DOI: 10.1021/acs.joc.7b00610
J. Org. Chem. 2017, 82, 6592−6603

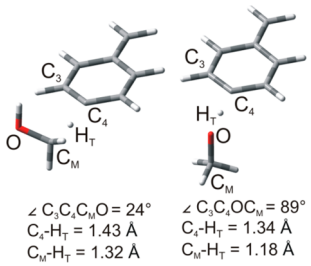

Figure 1. Transition state structures for the transfer of H−CH_2OH (left part) and H−OCH_3 (right part) to ^{3}**IIa**, taken as a model.

process. The results are gathered in Table 4, where both the overall free energy change (ΔG_{CASMP2}) and the free energy barrier ($\Delta G^{\ddagger}_{CASMP2}$) have been reported. The energy profiles along the whole IRC (100 steps in both directions) are plotted in Figures 2 and 3 for H-transfer from H−CH_2OH and H−OCH_3, respectively, in the case of ^{1,3}**IIa** (part a) and ^{1,3}**IIb** (part b). As for the C−H profile, the reaction is largely exergonic and the different isomers show similar behaviors, with $\Delta G^{\ddagger}$ values between ca. 13 and 19 kcal mol^{-1}. A similar scenario was found when considering the H transfer from the O−H position, where the reaction is again exergonic, although with less favorable energy changes. However, the observed $\Delta G^{\ddagger}$ values are very similar to the previous case (13 to 18 kcal mol^{-1} range). Apart from MeOH, we also evaluated the reactivity of ^{1,3}**IIb** at the H−$C(CH_3)_2OH$ position of isopropanol, since in the experiments we found a large amount of radical-type products when **1b** was irradiated in *i*PrOH/H_2O. Indeed, the model highlighted lower $\Delta G^{\ddagger}$ and more negative ΔG values with respect to the case of MeOH. Finally, we considered the case of the H−CH_2CN position in acetonitrile, for which we investigated the *para*- and *meta*-isomers only, since they show a ground state with different spin multiplicity (the triplet and the singlet, respectively). A more varied situation has been observed in this case, since, as far as the ground state is concerned, the *para*-isomer showed less favorable parameters with respect to the C−H of MeOH, while the opposite was true for the *meta*-one (Table 4).

Table 4. Calculated Parameters for the TSs Describing the Transfer of H from Solvent to IIa−c[a]

DHT	$\Delta G^{\ddagger}_{CASMP2}$ [kcal·mol^{-1}]	ΔG_{CASMP2} [kcal·mol^{-1}]
	reactivity at H−CH_2OH	
^{1}**IIa**	19.14	−23.06
^{3}**IIa**	**16.22**	**-13.50**
^{1}**IIb**	**16.12**	**-13.60**
^{3}**IIb**	12.79	−18.72
^{1}**IIc**	16.06	−24.00
^{3}**IIc**	**15.05**	**-14.28**
	reactivity at H−OCH_3	
^{1}**IIa**	14.05	−14.40
^{3}**IIa**	**15.77**	**-4.77**
^{1}**IIb**	**17.65**	−7.07
^{3}**IIb**	14.75	−8.69
^{1}**IIc**	13.32	−14.22
^{3}**IIc**	**16.34**	**-5.08**
	reactivity at H−$C(CH_3)_2OH$	
^{1}**IIb**	**9.59**	**-16.82**
^{3}**IIb**	8.49	−20.21
	reactivity at H−CH_2CN	
^{1}**IIa**	14.12	−21.91
^{3}**IIa**	**17.72**	**-9.92**
^{1}**IIb**	**13.77**	**-13.80**
^{3}**IIb**	13.83	−16.04

[a]The data referred to the most stable spin isomer have been reported in bold.

An interesting remark is related to the charge (q_{ESP} data have been reported; see also Computational Details) associated with the H atom during the transfer step (purple values in Figures 2 and 3). In the case of H−CH_2OH the charge always fell in the −0.1 to +0.1 range along the entire IRC (Figure 2). Some differences have been observed in the case of *i*PrOH and MeCN, where the charge of the H atom was slightly negative (around −0.15 at the TS; Figure S6) in the former case, while it assumed positive values (up to ca. + 0.2, particularly in the first part of the IRC; Figure S8) in the latter. Different was the case of the H−OCH_3 profiles, where a positive charge was associated with the H atom and it assumed much larger values (up to +0.5; Figure 3).

This charge localization is highly dependent on the O−H distance and decreases along the IRC, finally reaching the same values observed above for C−H around the end-points of the reaction path. Interestingly, we also verified that almost no charge localization occurred at the dicoordinated carbon atom, independently from the process and the isomer considered, with charge values ranging from −0.1 to +0.1 (gray values in Figures 2 and 3). The only exception to this trend is represented by the process describing the transfer of H−CH_2OH to **IIc**, where negative values (between −0.15 and −0.2) have been observed in the last part of the IRC (see Figure S2 for details).

Another issue is related to the starting point of the reported IRCs. Actually, we tried to optimize the corresponding structures to check for the formation, if any, of complexes between the DHTs and the molecule of solvent. Any attempt, however, failed and we never observed any coordination of methanol (either through the C−H or the O−H group) to the dicoordinated carbon of the DHT, independently from the isomer and spin considered.

As mentioned in the Introduction Section, the involvement of a zwitterionic intermediate to account for the reactivity observed in the case of **IIb** has been long debated in the literature.[22] Accordingly, we wanted to address this point in our simulation, with particular regards to the involvement of such electronic state during the H-transfer step from H−OCH_3. Thus, we took the geometries of the points along the IRC (from the starting point to the TS) reported in Figure 3b for ^{1}**IIb** and calculated the energy of the first excited state for each of them (see Section 2.5 in Supporting Information for details) to obtain a reaction profile describing the H atom transfer step along the excited state surface. The results are gathered in Figure 4, where it can be appreciated that the excited state profile lies ca. 50 kcal mol^{-1} above the IRC starting point of the ground state surface. Another interesting point is related to the charge associated with the H atom. It is noteworthy that less positive charge values are consistently observed along the excited state surface with respect to the ground state (purple values). This can be rationalized on the basis of a strong negative charge localization at the C_3 atom (the dicoordinated carbon) of ^{1}**IIb***, counterbalancing the electronegativity of the oxygen atom.

DOI: 10.1021/acs.joc.7b00610
J. Org. Chem. 2017, 82, 6592−6603

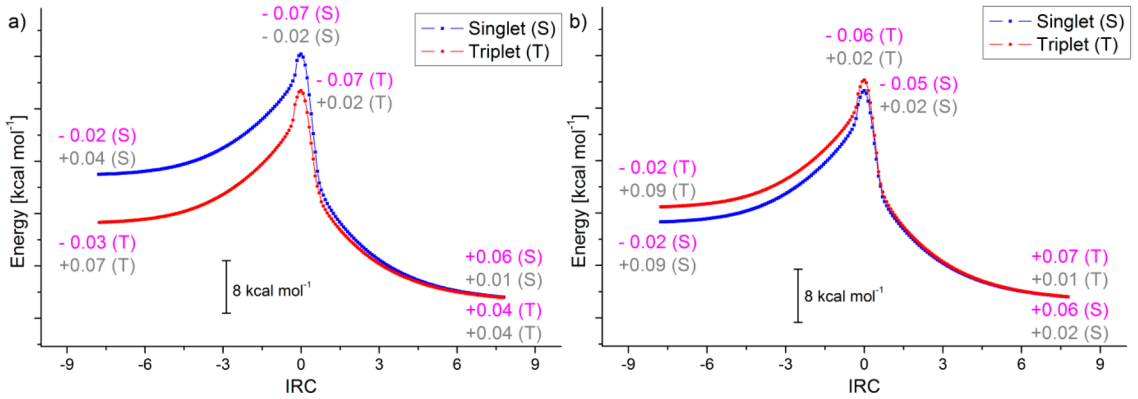

Figure 2. IRC plots of the TSs describing the reactivity of: (a) **IIa** and (b) **IIb** with methanol at the H−CH_2OH position ($E_{0(CASSCF,MeOH)}$ data have been reported, as detailed in Tables S5−S8; see Section 2.1). ESP charges (q_{ESP}) for H−CH_2OH and the dicoordinated carbon on relevant points (first, TS and last points) along the IRC are shown in purple and gray, respectively, as derived from the results of calculations at the CPCM-CASSCF/6-31G(d,p) level of theory in MeOH.

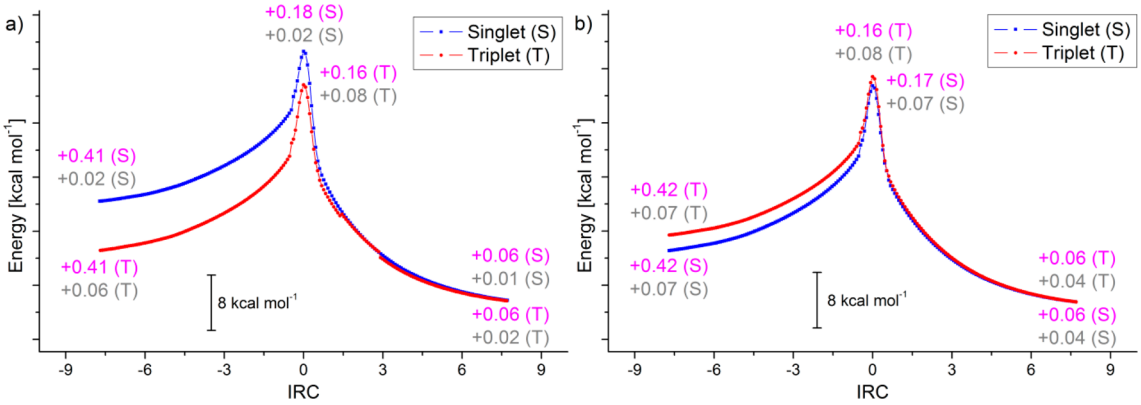

Figure 3. IRC plots of the TSs describing the reactivity of: (a) **IIa** and (b) **IIb** with methanol at the H−OCH_3 position ($E_{0(CASSCF,MeOH)}$ data have been reported, as detailed in Tables S11−S14; see Section 2.2). ESP charges (q_{ESP}) for H−OCH_3 and the dicoordinated carbon on relevant points (first, TS and last points) along the IRC are shown in purple and gray, respectively, as derived from the results of calculations at the CPCM-CASSCF/6-31G(d,p) level of theory in MeOH.

However, literature data indicates that zwitterionic ^{1}**IIb*** should lie ca. 30−40 kcal mol^{-1} (depending on the adopted theoretical approach) above the ground state,[22] much lower in energy than what found here. This could be due to our theoretical approach, based on single point calculations, thus providing vertical excitation energies and not a realistic scenario of the potential energy surface. Accordingly, we tried to optimize the structure of the excited DHT (^{1}**IIb***) in the presence of a MeOH molecule and, to our delight, we found a complex based on an interaction between the O−H moiety and the dicoordinated carbon of ^{1}**IIb***. The energy of this structure has been reported in Figure 4 (see the green circle) and was found to be much lower in energy, around 36 kcal mol^{-1} above the ground state, in accordance with the literature.[22] The structure of this complex (see geometry in Figure 4) also deserves some comments. First of all, the H−OCH_3 and C_3 carbon distance is around 2.0 Å, clearly highlighting an interaction between the two sites. Furthermore, the DHT skeleton is perfectly planar, but the hexagon ring is distorted, with a C_2−C_3−C_4 angle around 112°, and protrudes toward the MeOH molecule. Interestingly, this optimization also highlighted the formation of a partial negative charge (−0.48) at the dicoordinated carbon, confirming the different electronic distribution observed with respect to the ground state.

The above data do not account for the varied reactivity observed, since almost all of the isomeric DHTs offer very similar behaviors in the simulation system adopted. At the same time, the involvement of the zwitterionic excited state, despite being low in energy, seems not feasible. However, there are sparse reports in the literature highlighting the role of the solvent in tuning the reactivity of some intermediates, in particular of carbenes.[27] We mentioned above that the dicoordinated carbon (phenyl radical site) of ground state DHTs does not interact with the solvent. We surmised, however, that the situation could be different in the case of the benzylic position. Accordingly, we exposed the Cα atom of ^{1,3}**IIb** to the hydroxyl group of MeOH and tracked the effect of modifying the Cα-O distance on the resulting complex (see Section 2.6 in Supporting Information). The results are gathered in Figure 5 and it is important to highlight a marked difference between the singlet and the triplet state. In the latter case, we observed a monotonic behavior, with the energy increasing with the decrease of the Cα-O distance. Furthermore, the electronic structure of ^{3}**IIb** was not affected when approaching the hydroxyl group to the benzylic carbon. By contrast, in the ground state ^{1}**IIb**, both the geometry and the electronic structure were heavily affected. Three different stages can be observed. The first one concerns with a Cα-O distance ≥2.0 Å, where an energy variation around +30 kcal

DOI: 10.1021/acs.joc.7b00610
J. Org. Chem. 2017, 82, 6592−6603

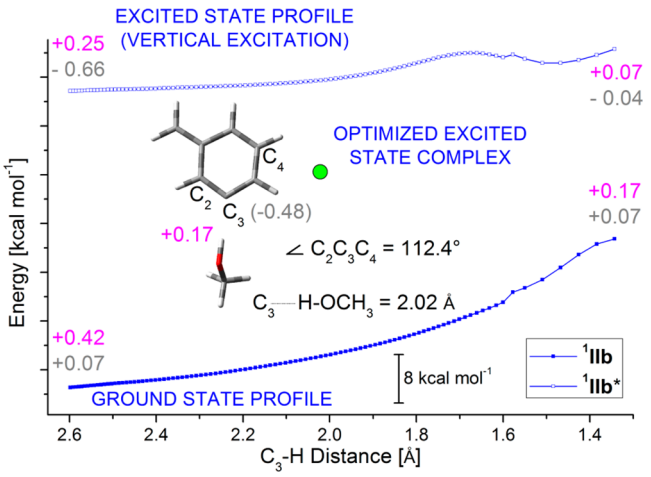

Figure 4. Reaction profile for the transfer of the H atom from H−OCH_3 to the dicoordinated carbon of ^{1}**IIb** on the ground state (solid symbols) and the excited state (open symbols) surfaces ($E_{0(CASSCF,MeOH)}$ data have been reported, as detailed in Table S23). ESP charges (q_{ESP}) for H−OCH_3 and the dicoordinated carbon (C_3) on relevant points (first and last points) along the reaction path are shown in purple and gray, respectively, as derived from the results of calculations at the CPCM-CASSCF/6-31G(d,p) level of theory in MeOH. The green circle indicates the position of the optimized structure (shown in the inset along with some relevant parameters) of the complex between ^{1}**IIb*** and MeOH.

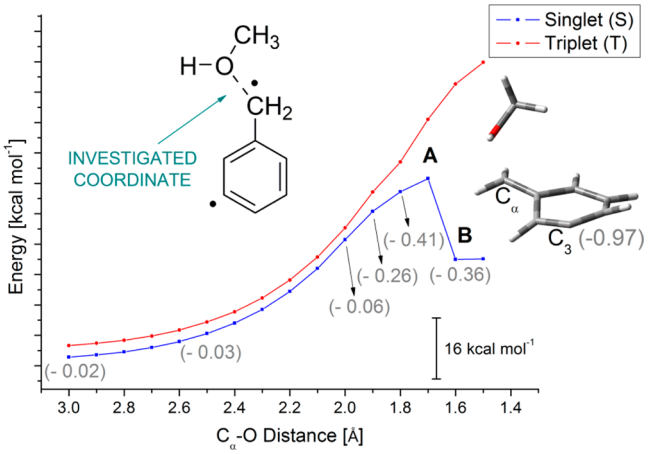

Figure 5. Energetic profile for the interaction of H−O−CH_3 with the Cα atom of ^{1,3}**IIb** ($E_{0(CASSCF,MeOH)}$ data have been reported, as detailed in Table S25). ESP charges (q_{ESP}) for the dicoordinated carbon (C_3) on relevant points are shown in gray, as derived from the results of calculations at the CPCM-CASSCF/6-31G(d,p) level of theory in MeOH. The structure shown corresponds to that of point **A**.

mol^{-1} was observed and the DHT structure remained planar with a peculiar diradical character ($\sigma^1\pi^1$ configuration, with two unpaired electrons and no charge localization). In the second region (1.7 Å < Cα-O distance <2.0 Å), the geometry started to deviate from planarity, with the C_2−C_3−C_4 moiety acquiring a sort of cumulenic character, and a partial negative charge developed at C_3. In the inset of Figure 5, the structure of point **A** has been reported, showing the highly distorted geometry observed in this region and highlighting the (almost) full negative charge located at C_3. In the third region (Cα-O distance ≤1.6 Å), a sharp discontinuity was observed (see point B) and the DHT structure assumed again a planar geometry, strictly resembling that reported above for excited state ^{1}**IIb***

(also showing a marked negative charge at the dicoordinated carbon).

A final simulation was undertaken to see the effect of the interaction of MeOH at the benzylic position on the TS describing the H atom transfer from H−OCH_3 to the dicoordinated carbon. The energetic profile is reported in Figure 6, where the energy of the TSs have been reported.

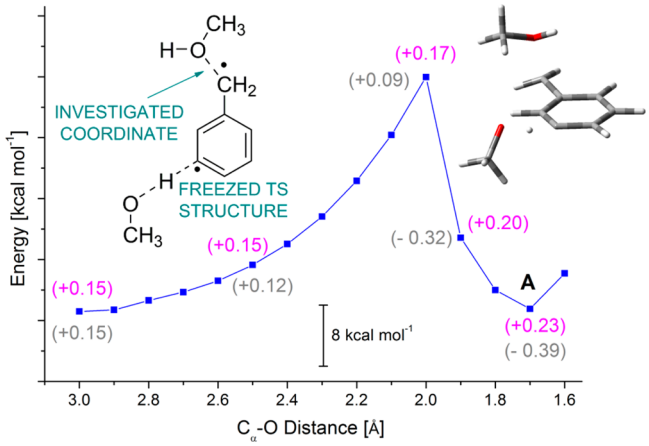

Figure 6. Energetic profile for the TSs describing the transfer of H−OCH_3 to the C_3 atom of ^{1}**IIb** as a function of the distance of the Cα atom to the hydroxyl group of a second Me−O-H molecule ($E_{0(CASSCF,MeOH)}$ data have been reported, as detailed in Table S26). ESP charges (q_{ESP}) for the exchanged H−OCH_3 and the C_3 atom on relevant points are shown in violet and gray, respectively, as derived from the results of calculations at the CPCM-CASSCF/6-31G(d,p) level of theory in MeOH. The structure shown corresponds to that of point **A**.

Interestingly, the profile was similar to that observed in Figure 5 and different regions can be extrapolated. In the first part (Cα-O distance ≥2.0 Å), the energy of the TSs increased with the decrease of the Cα-O distance, while small variations were observed both in terms of geometry (the DHT structure remains planar) and of charges associated with both the exchanged H atom and C_3 (a small positive value has been found in the latter case). By contrast, for Cα-O distance <2.0 Å, the energy of the TSs fell down and this discontinuity was accompanied by a marked change in terms of charges, particularly for the case of the C_3 atom, that acquired a partial negative charge (up to −0.39). As a result, the energy of the TS when the Cα-O distance was 1.7 Å, was comparable to that observed when the MeOH at the benzylic position was not interacting with the DHT (<0.5 kcal mol^{-1} difference; see the structure of point **A** reported in the inset of Figure 6). It is worth noting, however, that the course of the H atom transfer step was completely different, as testified by the different charges of C_3 involved.

DISCUSSION

The photoinduced generation of cations/diradicals from the examined chlorobenzylsilanes **1a−c** was carried out at room temperature and the mass balance of the products formed was decent in most cases. The products structure and distribution leave no doubt about the nature of the intermediates involved. As an example, the yields of products obtained in the photoinduced reactions of **1b** are comparable to those reported for reactions occurring via α,3-DHT under thermal conditions.[13] As mentioned in the Introduction, the generation of

DOI: 10.1021/acs.joc.7b00610
J. Org. Chem. 2017, 82, 6592−6603

DHTs reported here is a single photon, two steps process. The general features of the photoinduced heterolysis of chlorobenzenes via the triplet state are well-known,[28,29] as is the fact that a nucleophilic solvent (such as water) stabilizes the intermediate triplet phenyl cation,[19,23,24,30] thus favoring the occurrence of its peculiar reactions (e.g., hydrogen abstraction from the medium). However, cleavage of the C−Si bond may take place competitively, leading to the corresponding DHTs. Two intermediates were then mainly responsible of the variety of arylated derivatives formed, viz. the triplet cation (^{3}**VI**$^+$) and the DHT (**II**), as apparent from Tables 1−3.

From Triplet Phenyl Cations to *α,n*-DHTs. *Competing Processes.* The consumption of **1a−c** was significant (apart selected cases) in all of the protic media tested herein (Tables 1, 2), also when additives, such as tetrachloromethane or 1,4-cyclohexadiene, were present (Table 3). The desired desilylation to *α,n*-DHTs suffered, however, of competing chemistry[28,29,31] from the short-lived (a lifetime of 10 ns could be estimated)[32] triplet phenyl cations (^{3}**VI**$^+$**a−c**, Scheme 8).

Scheme 8. Reactivity of Triplet Phenyl Cations ^{3}VI$^+$a−c Photogenerated from 1a−c

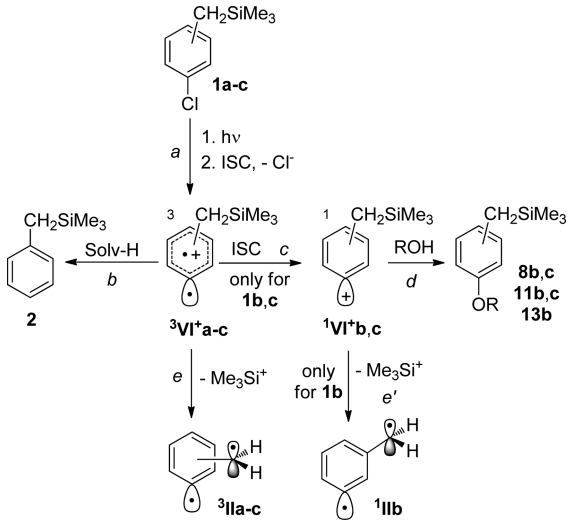

Accordingly, hydrogen abstraction from the solvent (Scheme 8, path b) took place significantly with the *ortho*- and *meta*-isomers. In these cases, the yield of benzylsilane **2** was in the 20 to 50% range, roughly following the BDE of the C−H bonds of the medium. Shifting from CH_3OH to CD_3OH led to the formation of **2**-d_1 supporting the involvement of a H(D) transfer from the CH_3/CD_3 group. In the case of the *ortho*- and *meta*-isomers **1b,c**, a minor process occurred since ISC from the first-formed triplets ^{3}**VI**$^+$**b,c** to the more stable singlet cations (^{1}**VI**$^+$**b,c**)[23a] allowed the isolation of solvolysis products **8b,c**, **11b,c** and **13b** (paths c,d). The generation of ^{1}**VI**$^+$**b**, however, opened an interesting route to singlet diradical ^{1}**IIb** (path e′). On the contrary, with the *para*-isomer **1a**, processes competitive with desilylation (path e) were always negligible, and reduction occurred only as a minor path (0−10%) even in the presence of excellent H-donors, such as CHD.

DHT Chemistry. According to what observed in our previous computational and experimental investigations,[19,23] desilylation of triplet ^{3}**VI**$^+$**a−c** and singlet (only for ^{1}**VI**$^+$**b**) phenyl cations to the corresponding ^{3}**IIa-c** or ^{1}**IIb**, respectively, (Scheme 8, paths e, e′) is a feasible process in protic media. Based on the present and previous computational evidence,[23a] DHTs are heterotopic diradical species (σ^1,π^1), with the two unpaired electrons not interacting, independently from the isomer and the spin state considered. However, they exhibit a different reactivity as demonstrated by the formation of polar products (such as benzyl alcohols and ethers) from *α*,3-DHT, initially assigned to a ionic mechanism rather than to a radical path.[18,20,22] Data in our hands suggest that all bare (i.e., not influenced by the medium where they are generated) DHTs are "purely diradical" species behaving in a similar way, and reaction occurs from the lowest-lying spin state for each isomer considered (see the bold data in Table 4). The more reactive site of the diradicals is the σ center, since the π center is stabilized by resonance.[26] Thus, hydrogen transfer (HT, Scheme 9, path a) operated by the phenyl radical site[26] from

Scheme 9. Reactivity of Photogenerated *α,n*-DHTs

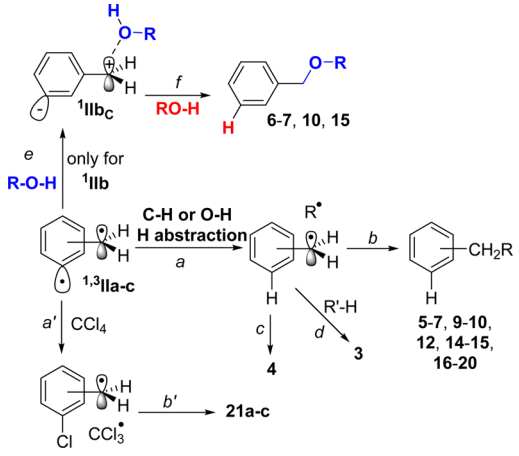

the solvent (ethers, acetonitrile and alcohols), as well as from CHD, was the first step and occurred preferentially at the C−H site.

The capability of aryl radicals in HT from the surrounding environment has been deeply investigated in the literature.[33] In alcohols, the rate constant for C−H cleavage occurring in primary C−H (BDE = 100.0 ± 2.0 kcal mol^{-1})[34] of *tert*-butanol was measured to be up to 30 times slower than from labile *α*-oxy C−H bond (91 ± 1.0 kcal mol^{-1})[34] in isopropanol[35] for which C−H cleavage occurred exclusively. On the other hand, in methanol both the C−H (96.0 ± 0.1 kcal mol^{-1})[34] and O−H (104.2 ± 0.9 kcal mol^{-1})[34] bonds were cleaved with a ratio of ca. 9:1.[36] Analogously, in ethanol and *t*BuOH, a competitive hydrogen transfer from O−H and C−H bonds occurred, depending on both statistics and thermodynamic effects. Moreover, hydrogen abstraction by phenyl radical was described as slightly exothermic (4.2 kcal mol^{-1}) also from water and observed in a few experiments at low-temperature in argon matrices.[37]

The computational data reported in Table 4 highlight that DHTs can abstract efficiently both electrophilic (from CH_3CN, BDE C−H = 96 kcal mol^{-1})[34] and nucleophilic (from the C−H positions of alcohols) hydrogens thanks to the reactivity imparted by the phenyl radical site. Experimental data in our hands pointed out that *α*-hydrogens in ethers (e.g., THF, BDE = 92.1 ± 1.6 kcal mol^{-1})[34] were selectively extracted. Turning to the C−H vs O−H competition for the case of CH_3OH, very similar activation parameters have been found in the present simulation, making a generalization unfeasible. This topic has

DOI: 10.1021/acs.joc.7b00610
J. Org. Chem. 2017, 82, 6592−6603

been already debated in the literature, since theoretical simulations, showing a preference for the O−H abstraction, were apparently in disagreement with experimental data.[22] The reason for this failure was however found in an inaccurate handling of hydrogen bonding by the simulation adopted and ruled out the possibility that the α,3-DHT diradical could react with the O−H site.[22] We propose, however, that all DHTs can promote both reactivities through a homolytic mechanism, with a preference toward the C−H vs the O−H site (see data gathered in Table 4). This is evident by analyzing the data for **1a**, where we can surmise that the only responsible for the observed DHT-deriving products is ^{3}**IIa**. Actually, we observed a decrease of the radical/polar products ratio when the BDE of the C−H bond of the solvent increases. This is particularly clear if we consider the results from the experiments carried out in *t*BuOH and in CD_3OH. The experiments in deuterated solvents further support the fact that HT occurs from the O−H or the C−H, respectively, in the formation of polar and radical products, according to the deuteration pattern observed on the aromatic ring. As depicted in Scheme 9, this HT event leads to benzyl radicals (path a), that upon coupling with the radicals arising from the solvent, are responsible for the formation of alcohols **5**, **7**, **9**, **12**, **14**; benzyl ethers **6**, **10**, **15**; and products **16**−**20** (path b). Benzyl radicals can also dimerize to bibenzyl **4** (path c), as well as abstract a hydrogen (path d) to yield toluene **3**. HT also occurs from 1,4-CHD, and coupling of the generated radicals affords alkyl benzene **19**.

Chlorine abstraction from CCl_4 followed by coupling of the resulting benzyl/$Cl_3C^\bullet$ radical pair (paths a′, b′) affords tetrachlorinated aromatics **21a**−**c**[18a] (notice that radical products **4** and **5** are not formed in the presence of such additive). However, though both polar and radical products can be observed via a radical pathway, the latter will be predominant, since homolytic cleavage of a C−H bond always requires a lower energy than to cleave an O−H bond.

Very similar conclusions can be drawn for **1c**, while the product distribution is completely different for **1b**, despite the similar computational results obtained for **IIb**. In our opinion, this different behavior can be ascribed to the fact that **IIb** is the only isomer showing a singlet ground state. Indeed, the peculiar behavior of singlet DHTs has been previously shown to have some generality, as demonstrated in the case of methoxy-substituted α,*n*-DHTs.[23b] Turning to the computational results, it is worth noting that the pathways previously described apply for bare DHTs only (Scheme 9, path a), while the situation may be different if a suitable model able to appreciate specific interactions with the nucleophilic solvent is considered. Thus, forcing the MeOH molecule to coordinate at the benzylic site causes a charge separation in ^{1}**IIb**, tagged as complexed ^{1}**IIb** (^{1}**IIb**$_C$ in Scheme 9) with the development of a (partial) negative charge at the dicoordinated carbon, and renders it similar to the first excited state ^{1}**IIb***. It is no surprise that both Figures 5 and 6 show a sharp discontinuity, because in both cases the approach of the lone pair of oxygen of MeOH to the benzylic position causes an electronic reorganization, ultimately leading to the population of the excited state of ^{1}**IIb** (and in turn causing the observed discontinuity). In our opinion, however, this is not the most important part of Figures 5 and 6, while it should be highlighted the behavior observed in the points with a Cα-O distance in the 1.8−2.0 Å range, where it is demonstrated that a charge separation in ^{1}**IIb** is actually feasible. The present model is obviously approximated and shows that such coordination occurs with an energy increase. However, we believe that several MeOH molecules could concur to this interaction (in turn, facilitating it) and that a continuum of situations may arise (without arriving at the extreme case involving the formation of the excited state), where the development of the negative charge is strictly related with the extent of the interaction of the solvent at the benzylic position. Such charge-separated species, as previously suggested,[22] can form polar products (such as benzyl ethers **6**, **10**, **15**, and benzyl alcohol **7**) through an ionic addition mechanism. Furthermore, it is interesting to highlight that such polarization can operate on singlet species only, in strict accordance with experimental results. A zwitterion reactivity is thus effectively present in the case of chloride **1b**. Thus, in the presence of H donors such as isopropanol or CHD, a radical behavior arising from bare ^{1}**IIb** is the main or even the only observed, whereas, when using *t*BuOH/water mixture as the medium as well as in the presence of deuterated CD_3OH, we have a chance to observe the reactivity of ^{1}**IIb**$_C$, which afforded polar products in amounts larger than those observed for other isomers. Similarly, Carpenter et al. proposed, in the case of thermally generated α,3-DHT, a nonadiabatic surface crossing from the ground state to the first excited-state zwitterionic singlet surface.[22]

A similar behavior was described by Sander when investigating the ground state of diphenylcarbene.[27a] However, in that case a hydrogen bonding with the solvent caused an inversion of the ground state of the intermediate, whereas in the present investigation the nucleophilic site of the medium caused the formation of a charge-separated species, strictly resembling the effect of the excitation from S_0 to S_1 in ^{1}**IIb**. The nucleophilic addition to a radical center in other aromatic diradicals has been also investigated (by having recourse to both computational and experimental analyses) as in the case of *para*-benzynes, in order to explain the biosynthetic pathway to cyanosporasides,[10] where the formal addition of HCl onto a 1,4-didehydrobenzene has been observed. In that case, the reaction took place with an energy barrier largely due to the solvation of the nucleophile, and nucleophilic addition was followed by protonation.

■ CONCLUSIONS

Since the discovery of the Myers-Saito cycloaromatization of enyne-allenes, the competing diradical/zwitterion reactivity of didehydrotoluenes has been the object of detailed investigations, most of them limited by the exclusive accessibility of the α,3-isomer under thermal conditions. The photochemical approach adopted in the present study allowed the generation of all of the DHT isomers and highlighted the dependence of the reactivity of diradicals on the actual spin state involved. Thus, bare α,*n*-DHT intermediates exhibit a unique diradical reactivity responsible for the formation of radical and polar products (the latter in a minor amounts), whereas interaction of singlet α,3-isomer with the solvent resulted in the formation of a polarized species (termed "complexed DHT"), which allowed for the formation of polar compounds.

■ EXPERIMENTAL SECTION

General Considerations. ^{1}H NMR spectra were recorded with a 300 MHz spectrometer, while ^{13}C NMR spectra were recorded with a 75 MHz spectrometer. The attributions were made on the basis of ^{1}H and ^{13}C NMR, as well as DEPT-135 experiments; chemical shifts are reported in ppm downfield from TMS. GC-MS analyses were carried out using a Thermo Scientific DSQII single quadrupole GC/MS

DOI: 10.1021/acs.joc.7b00610
J. Org. Chem. 2017, 82, 6592−6603

system. A Restek Rtx-5MS (30 m × 0.25 mm × 0.25 μm) capillary column was used for analytes separation with helium as carrier gas at 1 mL min^{-1}. The injection in the GC system was performed in split mode and the injector temperature was 250 °C. The GC oven temperature was held at 60 °C for 5 min, increased to 250 °C by a temperature ramp of 10 °C min^{-1}, and held for 10 min. The transfer line temperature was 270 °C and the ion source temperature 250 °C. Mass spectral analyses were carried out in full scan mode.

The employed solvents (acetonitrile, water, methanol, ethanol, and isopropanol) were of HPLC purity. *tert*-Butanol, tetrahydrofuran, 1,4-dioxane, CCl_4, and 1,4-cyclohexadiene (reagent grade) were freshly distilled before use. Compounds **1a**–**c**[19] have been synthesized by following a known procedure. The amounts of **2**–**7**, **8b**,**c**,[25] **9**, **10**,[38] **12**, **14**, **15**,[39,40] **18**, and **20**[41] have been determined on the basis of calibration curves by comparison with either commercial standards or synthesized compounds. Compounds **13b**, **19**,[18a] **21a**, and **21c** have been identified and quantified on the basis of GC-MS analyses (see Table S1 for further details).

*(3-Isopropyloxybenzyl)trimethylsilane (**11b**).* The title compound was prepared by adapting a procedure described for the synthesis of 5-methoxy-1,3-benzodioxole.[42] A mixture of **8b**[25] (1.0 g, 5.5 mmol) and K_2CO_3 (0.40 g, 2.9 mmol) in acetone (34 mL) was stirred for 30 min, then 2-bromopropane (42 mmol) was added dropwise and the resulting mixture was refluxed for 48 h. After the mixture was cooled to room temperature, water (20 mL) was added and the mixture was extracted with diethyl ether (3 × 20 mL), the organic phases were reunited, dried over $MgSO_4$, and then concentrated. Purification of the crude product by column chromatography (eluant: neat cyclohexane) afforded 0.13 g of **11b** (oil, 11% yield). **11b**: ^{1}H NMR ($CDCl_3$, 300 MHz) δ 0.05 (s, 9H), 1.35–1.40 (d, 6H, *J* = 6 Hz), 2.08 (s, 2H), 4.50–4.55 (m, 1H), 6.55–6.60 (m, 3H), 7.10–7.15 (m, 1H). ^{13}C NMR ($CDCl_3$, 75 MHz) δ −1.9 (CH_3), 22.0 (CH_3), 27.1 (CH_2), 69.6 (CH), 111.4 (CH), 115.7 (CH), 120.4 (CH), 128.9 (CH), 142.0, 157.7. IR (ν, cm^{-1}): 3028, 2956, 1597, 1485, 1258, 1157, 851. MS (*m*/*z*): 222 (M^+, 5), 189 (10), 132 (50), 117 (55), 104 (38), 91 (26), 73 (100).

*1-Chloro-3-(2,2,2-trichloroethyl)benzene (**21b**).* Compound **21b** was obtained by adapting a procedure for the synthesis of **20**.[41] $CHCl_3$ (1.9 mL, 24 mmol) was added dropwise to a cooled (0 °C) solution of NaH (60% dispersion in mineral oil, 0.5 g, 12 mmol) in dry DMF (30 mL). 3-Chlorobenzyl bromide (0.5 mL, 3.8 mmol) was thus added dropwise and the solution stirred for 15 h. The reaction mixture was poured over ice (50 g) and extracted with hexane (3 × 50 mL). The organic phases were reunited, dried over $MgSO_4$, and concentrated. Purification of the crude product by column chromatography (eluant: neat hexane) afforded 0.12 g of **21b**[43] (oil, 13% yield). **21b**: ^{1}H NMR ($CDCl_3$, 300 MHz) δ 3.93 (s, 2H), 7.30–7.40 (m, 4H), 7.45–7.50 (m, 1H). ^{13}C NMR ($CDCl_3$, 75 MHz) δ 59.1 (CH_2), 98.1, 128.5 (CH), 129.3 (CH), 129.7 (CH), 131.5 (CH), 133.9, 134.9. IR (ν, cm^{-1}): 3067, 2926, 1575, 1082, 955, 805. MS (*m*/*z*): 244 (M^+, 12), 207 (10), 136 (9), 127 (32), 125 (100), 89 (8), 75 (7).

Photochemical Experiments. The photochemical reactions were performed by using nitrogen-purged solutions of **1a**–**c** (0.025 M) in the chosen medium in quartz tubes. Irradiations were performed in a multilamp reactor fitted with 10 × 15 W phosphor-coated lamps (maximum of emission at 310 nm). The reaction course was followed by means of GC and GC-MS analyses. Workup of the irradiated mixtures involved concentration in vacuo and chromatographic separation by using silica gel as stationary phase. Quantum yields were measured at 254 nm (1 Hg lamp, 15W).

*Irradiation of **1a** in a Tetrahydrofuran/Water 2:1 Mixture.* A degassed solution of **1a** (149 mg, 0.75 mmol, 0.025 M) in a THF/H_2O 2:1 mixture (30 mL) was irradiated for 15 h at 310 nm. The photolyzed solution was then extracted with diethyl ether (3 × 20 mL), the organic phases were reunited, dried over $MgSO_4$, and concentrated. Purification of the residue by column chromatography (eluant: neat hexane) afforded 74 mg of 2-benzyltetrahydrofuran (**16**, 61% yield). GC analysis of the irradiated solution revealed also the presence of benzyltrimethylsilane (**2**, 10% yield) and 1,2-diphenylethane (**4**, 11% yield). Spectroscopic data of **16** were in accordance with the literature.[44]

*Irradiation of **1a** in a 1,4-Dioxane/Water 2:1 Mixture.* A degassed solution of **1a** (149 mg, 0.75 mmol, 0.025 M) in a 1,4-dioxane/H_2O 2:1 mixture (30 mL) was irradiated for 15 h at 310 nm. The photolyzed solution was then extracted with diethyl ether (3 × 20 mL), dried over $MgSO_4$, and concentrated. Purification of the residue by column chromatography (eluant: neat hexane) afforded 88 mg of 2-benzyl-1,4-dioxane (**17**, 66% yield).[45] GC analysis of the solution revealed also the presence of benzyltrimethylsilane (**2**, 4% yield) and 1,2-diphenylethane (**4**, 10% yield). **17**: ^{1}H NMR ($CDCl_3$, 300 MHz) δ 2.60–2.80 (AB part of an ABX system, 2H), 3.35–3.40 (X' part of an A'B'X' system, 1H), 3.65–3.85 (m, 6H), 7.20–7.35 (m, 5H). ^{13}C NMR ($CDCl_3$, 75 MHz) δ 38.3 (CH_2), 66.3 (CH_2), 66.8 (CH_2), 70.8 (CH_2), 76.0 (CH), 126.4 (CH), 128.3 (CH), 129.1 (CH), 137.3. IR (ν, cm^{-1}): 3028, 2596, 1122, 700. MS (*m*/*z*): 178 (M^+, 3), 117 (6), 92 (10), 91 (55), 87 (100), 86 (68), 65 (15), 59 (7), 43 (16).

Computational Methods. All the calculations were carried out using the Gaussian 09 program package.[46] In our investigation, the optimization of all of the stationary points was carried out with the CASSCF (complete active space self-consistent field) method by using the standard 6-31G(d,p) basis set. No symmetry constraint was applied to the investigated structures. The occupancies of the orbitals included in the active space were carefully checked, and the values observed were always higher than 0.01 and lower than 1.99 for all of the stationary points reported, as recommended.[46] Frequency calculations were performed in vacuo to check the nature of the located stationary points. In particular, it was verified that minima had no imaginary frequencies, while transition states (TS) showed one imaginary frequency, describing the reaction coordinate of interest. For each reacting situation, a systematic investigation on all of the possible conformations at the TS level has been carried out. However, since the difference in energy of these optimized structures was small (in most cases, < 1 kcal·mol^{-1}), only the most stable conformation has been reported and has been considered for further work. The solvent effect was included by single-point calculations at the CPCM-CASSCF/6-31G(d,p) method (methanol, isopropanol, or acetonitrile bulk) on the optimized geometries obtained in vacuo.[47] The solvent cavity was calculated using the united atom topological model applied on radii optimized for the HF/6-31G(d) level of theory (RADII = UAHF option). Atomic charges have been calculated in solvent bulk according to the Merz–Singh–Kollman scheme,[48] via the POP = MK keyword and have been labeled in the text as "q_{ESP}". MP2 corrections have been calculated by single-point calculations at the CASSCF-MP2/6-31G(d,p) level on the optimized geometries obtained in vacuo, adopting a configuration threshold equal to 0.05 via the IOP (5/52 = 20) option. The CASMP2/6-31G(d,p) Gibbs free energies reported in Table S3 have thus been calculated by means of eq 1 reported below, in analogy with previous works by our group.[23]

$$G_{CASMP2} = E_{0(CASSCF,CPCM)} + \Delta E_{CORR(MP2,vacuo)} + \Delta G_{CORR(vacuo)} \quad (1)$$

Where $E_{0(CASSCF,CPCM)}$ is the total electronic energy calculated at the CPCM-CASSCF level (methanol, isopropanol, or acetonitrile bulk); $\Delta E_{CORR(MP2,vacuo)}$ is the MP2 correction calculated in vacuo on the geometry previously optimized; $\Delta G_{CORR(vacuo)}$ is the unscaled thermal correction to Gibbs free energy as from the output of the frequency calculation in vacuo, also including the zero-point vibrational energy (ZPVE). The single terms contributing to the determination of G_{CASMP2} values have been gathered in Table S4.

The detailed characterization of TSs has been performed via the IRC method at the same level of theory as the optimizations (CASSCF/6-31G(d,p)) by describing 100 points in each direction (100 points in the forward and 100 points in the reverse direction). Also in this case, solvent effects were included via single point calculations on each of the optimized points along the IRC, as described above. The description of IRC profiles has been carried out by plotting $E_{0(CASSCF,CPCM)}$ vs the reaction coordinate. Indeed, it was considered that the first and last points gave a good approximation of the starting and final reacting situations, respectively, since a very

DOI: 10.1021/acs.joc.7b00610
J. Org. Chem. 2017, 82, 6592–6603

smooth profile was observed. The thermodynamic parameters reported in Tables 4 and S3, viz. ΔG_{CASMP2} and $\Delta G^{\ddagger}_{CASMP2}$, have thus been determined according to eqs 2 and 3 reported below:

$$\Delta G_{CASMP2} = G_{CASMP2}(\text{IRC end-point}) - G_{CASMP2}(\text{IRC start-point}) \quad (2)$$

$$\Delta G^{\ddagger}_{CASMP2} = G_{CASMP2}(\text{TS}) - G_{CASMP2}(\text{IRC start-point}) \quad (3)$$

As for the active spaces chosen, we routinely adopted a (10,10) approach, where the orbitals considered were the 3 π and the 3 π^* orbitals of the aromatic ring, the orbital at the dicoordinated carbon and the orbital at the benzylic position, and the σ/σ^* couple of the relevant bond to be broken along the reaction coordinate. In some instances, however, slight modifications to this approach have been applied, as detailed in each section of the SI. Slight variations to the definition of the terms above have been introduced, according to the compounds under investigation; for details, see the sections of each class of molecules in the SI. Optimized geometry listed in Cartesian format (coordinates are given in Å), minimum energies and thermochemical data (in Hartree; the default options were adopted in the latter case, viz. temperature: 298.150 K and pressure: 1.00000 atm) are reported in the SI. The conversion factor between Hartree and kcal mol^{-1} has been: 1 hartree = 627.509 kcal mol^{-1}. When summing the data for calculating G_{CASMP2} (see eq 1), all the digits available from the calculations were used; nevertheless, the energy values reported (in Hartree units) have been rounded considering 6 significant digits after the unit.

■ ASSOCIATED CONTENT

Supporting Information

The Supporting Information is available free of charge on the ACS Publications website at DOI: 10.1021/acs.joc.7b00610.

Experimental details, sample spectra, optimized geometries, energies, and CASSCF output data for all of the structures involved in this work (PDF)

■ AUTHOR INFORMATION

Corresponding Authors

*E-mail: davide.ravelli@unipv.it; Fax: +39 0382 987323; Tel: +39 0382 987198.

*E-mail: fagnoni@unipv.it; Fax: +39 0382 987323; Tel: +39 0382 987198.

ORCID

Davide Ravelli: 0000-0003-2201-4828

Maurizio Fagnoni: 0000-0003-0247-7585

Notes

The authors declare no competing financial interest.

■ ACKNOWLEDGMENTS

This work was supported by the Fondazione Cariplo (grant 2011-1839). We are grateful to Dr. B. Mannucci and Dr. F. Corana (Centro Grandi Strumenti, Pavia) for the valuable assistance. We thank Dr. C. Raviola and Dr. S. Crespi (University of Pavia) for fruitful discussions. This work was funded by the CINECA Supercomputer Center, with computer time granted by ISCRA projects (code: HP10CN4237 and HP10CSWWDQ).

■ REFERENCES

(1) Peterson, P. W.; Mohamed, R. K.; Alabugin, I. V. *Eur. J. Org. Chem.* **2013**, *2013*, 2505−2527.

(2) Sankararaman, S. *Pericyclic Reactions - A Textbook: Reactions, Applications and Theory*; Wiley-VCH: Weinheim, 2005.

(3) Abe, M. *Chem. Rev.* **2013**, *113*, 7011−7088.

(4) Albini, A.; Fagnoni, M. *Photochemically-generated intermediates in synthesis*; John Wiley & Sons: Hoboken, 2013; pp 131−167.

(5) Mohamed, R. K.; Peterson, P. W.; Alabugin, I. V. *Chem. Rev.* **2013**, *113*, 7089−7129.

(6) (a) Jones, R. R.; Bergman, R. G. *J. Am. Chem. Soc.* **1972**, *94*, 660−661. (b) Bergman, R. G. *Acc. Chem. Res.* **1973**, *6*, 25−31.

(7) Kraka, E.; Cremer, D. *WIREs Comput. Mol. Sci.* **2014**, *4*, 285−324.

(8) Alabugin, I.; Breiner, B.; Manoharan, M. *Adv. Phys. Org. Chem.* **2007**, *42*, 1−33.

(9) (a) Raviola, C.; Protti, S.; Ravelli, D.; Fagnoni, M. *Chem. Soc. Rev.* **2016**, *45*, 4364−4390. (b) Wang, K. K. *Chem. Rev.* **1996**, *96*, 207−222.

(10) (a) Perrin, C. L.; Reyes-Rodríguez, G. J. *J. Phys. Org. Chem.* **2013**, *26*, 206−210. (b) Yamada, K.; Lear, M. J.; Yamaguchi, T.; Yamashita, S.; Gridnev, I. D.; Hayashi, Y.; Hirama, M. *Angew. Chem., Int. Ed.* **2014**, *53*, 13902−13906. (c) dos Passos Gomes, G.; Alabugin, I. V. *J. Am. Chem. Soc.* **2017**, *139*, 3406−3416.

(11) Wenthold, P. G.; Wierschke, S. G.; Nash, J. J.; Squires, R. R. *J. Am. Chem. Soc.* **1994**, *116*, 7378−7392.

(12) Experimental and early computational investigation of triplet diradicals including $^3\alpha$,3-DHT and fulvene triplet diradicals has been also carried out by Schmittel and co-workers, see for instance Bucher, G.; Mahajan, A. A.; Schmittel, M. *J. Org. Chem.* **2009**, *74*, 5850−5860. Schmittel, M.; Mahajan, A. A.; Bucher, G. *J. Am. Chem. Soc.* **2005**, *127*, 5324−5325. Bucher, G.; Mahajan, A. A.; Schmittel, M. *J. Org. Chem.* **2008**, *73*, 8815−8828.

(13) See for instance: (a) Myers, A. G.; Parrish, C. A. *Bioconjugate Chem.* **1996**, *7*, 322−331. (b) Lin, C.-F.; Wu, M.-J. *J. Org. Chem.* **1997**, *62*, 4546−4548. (c) Suzuki, I.; Tsuchiya, Y.; Shigenaga, A.; Nemoto, H.; Shibuya, M. *Tetrahedron Lett.* **2002**, *43*, 6779−6781. (d) Suzuki, I.; Uno, S.; Tsuchiya, Y.; Shigenaga, A.; Nemoto, H.; Shibuya, M. *Bioorg. Med. Chem. Lett.* **2004**, *14*, 2959−2962. (e) Kuzmin, A. V.; Popik, V. V. *Chem. Commun.* **2009**, 5707−5709. (f) Nicolaou, K. C.; Skokotas, G.; Furuya, S.; Suemune, H.; Nicolaou, D. C. *Angew. Chem., Int. Ed. Engl.* **1990**, *29*, 1064−1067.

(14) Nagata, R.; Yamanaka, H.; Okazaki, E.; Saito, I. *Tetrahedron Lett.* **1989**, *30*, 4995−4998.

(15) (a) Smith, A. L.; Nicolaou, C. *J. Med. Chem.* **1996**, *39*, 2103−2117. (b) *Enediyne Antibiotics as Antitumor Agents Borders*; D, B., Doyle, T. W., Eds; Marcel Dekker: New York, 1995.

(16) Suzuki, I.; Shigenaga, A.; Manabe, A.; Nemoto, H.; Shibuya, M. *Tetrahedron* **2003**, *59*, 5691−5704.

(17) Kar, M.; Basak, A. *Chem. Rev.* **2007**, *107*, 2861−2890.

(18) (a) Myers, A. G.; Kuo, E. Y.; Finney, N. S. *J. Am. Chem. Soc.* **1989**, *111*, 8057−8059. (b) Myers, A. G.; Dragovich, P. S. *J. Am. Chem. Soc.* **1989**, *111*, 9130−9132. (c) Nagata, R.; Yamanaka, H.; Murahashi, E.; Saito, I. *Tetrahedron Lett.* **1990**, *31*, 2907−2910. (d) Myers, A. G.; Dragovich, P. S.; Kuo, E. Y. *J. Am. Chem. Soc.* **1992**, *114*, 9369−9386.

(19) Protti, S.; Ravelli, D.; Mannucci, B.; Albini, A.; Fagnoni, M. *Angew. Chem., Int. Ed.* **2012**, *51*, 8577−8580.

(20) Hughes, T. S.; Carpenter, B. K. *J. Chem. Soc., Perkin Trans. 2* **1999**, 2291−2298.

(21) Engels, B.; Hanrath, M. *J. Am. Chem. Soc.* **1998**, *120*, 6356−6361.

(22) Cremeens, M. E.; Hughes, T. S.; Carpenter, B. K. *J. Am. Chem. Soc.* **2005**, *127*, 6652−6661.

(23) (a) Ravelli, D.; Protti, S.; Fagnoni, M.; Albini, A. *J. Org. Chem.* **2013**, *78*, 3814−3820. (b) Raviola, C.; Ravelli, D.; Protti, S.; Fagnoni, M. *J. Am. Chem. Soc.* **2014**, *136*, 13874−13881.

(24) Ravelli, D.; Protti, S.; Fagnoni, M. *J. Org. Chem.* **2015**, *80*, 852−858.

(25) Crespi, S.; Ravelli, D.; Protti, S.; Albini, A.; Fagnoni, M. *Chem. - Eur. J.* **2014**, *20*, 17572−17578.

(26) Liu, B.; Wang, K. K.; Petersen, J. L. *J. Org. Chem.* **1996**, *61*, 8503−8507.

DOI: 10.1021/acs.joc.7b00610
J. Org. Chem. 2017, 82, 6592−6603

(27) (a) Costa, P.; Sander, W. *Angew. Chem., Int. Ed.* **2014**, *53*, 5122−5125. (b) Tomioka, H.; Ozaki, Y.; Izawa, Y. *Tetrahedron* **1985**, *41*, 4987−4993.
(28) (a) Raviola, C.; Ravelli, D.; Protti, S.; Albini, A.; Fagnoni, M. *Synlett* **2015**, *26*, 471−478. (b) Bondarchuk, S. V.; Minaev, B. F. *J. Phys. Chem. A* **2014**, *118*, 3201−3210. (c) Rayne, S.; Forest, K. *Theor. Chem. Acc.* **2016**, *135*, 69.
(29) Dichiarante, V.; Protti, S.; Fagnoni, M. *J. Photochem. Photobiol., A* **2017**, *339*, 103−113.
(30) Protti, S.; Dichiarante, V.; Dondi, D.; Fagnoni, M.; Albini, A. *Chem. Sci.* **2012**, *3*, 1330−1337.
(31) (a) Qrareya, H.; Raviola, C.; Protti, S.; Fagnoni, M.; Albini, A. *J. Org. Chem.* **2013**, *78*, 6016−6024. (b) Dichiarante, V.; Salvaneschi, A.; Protti, S.; Dondi, D.; Fagnoni, M.; Albini, A. *J. Am. Chem. Soc.* **2007**, *129*, 15919−15926.
(32) Manet, I.; Monti, S.; Grabner, G.; Protti, S.; Dondi, D.; Dichiarante, V.; Fagnoni, M.; Albini, A. *Chem. - Eur. J.* **2008**, *14*, 1029−1039.
(33) See for instance: (a) Pryor, W. A.; Echols, J. V., Jr.; Smith, K. *J. Am. Chem. Soc.* **1966**, *88*, 1189−1199. (b) Kopinke, F.-D.; Zimmermann, G.; Anders, K. *J. Org. Chem.* **1989**, *54*, 3571−3576. (c) Jing, L.; Guler, L. P.; Pates, G.; Kenttämaa, H. I. *J. Phys. Chem. A* **2008**, *112*, 9708−9715. (d) Galli, C. *Chem. Rev.* **1988**, *88*, 765−792. (d1) Logan, C. F.; Chen, P. *J. Am. Chem. Soc.* **1996**, *118*, 2113−2114.
(34) Luo, Y. R. *Handbook of Bond Dissociation Energies in Organic Compounds*; CRC Press: Boca Raton, 2003.
(35) Fang, X.; Mertens, R.; von Sonntag, C. *J. Chem. Soc., Perkin Trans. 2* **1995**, 1033−1036.
(36) König, E.; Musso, H.; Zàhorsky, U.-I. *Angew. Chem., Int. Ed. Engl.* **1972**, *11*, 45.
(37) Mardyukov, A.; Sanchez-Garcia, E.; Crespo-Otero, R.; Sander, W. *Angew. Chem., Int. Ed.* **2009**, *48*, 4804−4807.
(38) Gellert, B. A.; Kahlcke, N.; Feurer, M.; Roth, S. *Chem. - Eur. J.* **2011**, *17*, 12203−12209.
(39) Strazzolini, P.; Runcio, A. *Eur. J. Org. Chem.* **2003**, *2003*, 526−536.
(40) Spectroscopic data for compound **15** were in accordance with literature: Xu, Q.; Xie, H.; Chen, P.; Yu, L.; Chen, J.; Hu, X. *Green Chem.* **2015**, *17*, 2774−2779 MS (m/z): 164 (M^+, 5), 149 (15), 92 (8), 91 (100).
(41) Baati, R.; Barma, D. K.; Murali Krishna, U.; Mioskowski, C.; Falck, J. R. *Tetrahedron Lett.* **2002**, *43*, 959−961 Spectroscopic data for **20**: ^{1}H NMR ($CDCl_3$, 300 Hz) 3.98 (s, 2H), 7.40−7.45 (m, 3H), 7.50−7.55 (m, 2H); 13C NMR 58.7 (CH_2), 98.9, 128.1 (CH), 128.3 (CH), 131.6 (CH), 133.2. IR (ν cm^{-1}): 3030, 2950, 1497, 1455, 1206, 1080, 853. MS (m/z): 212 (3), 209 (M^+,9), 208 (11), 92 (10), 91 (100).
(42) Barrero, F.; Alvarez-Manzaneda, E. J.; Chahboun, R. *Tetrahedron* **1998**, *54*, 5635−5650.
(43) Ando, A.; Miki, T.; Kumadaki, I. *J. Org. Chem.* **1988**, *53*, 3637−3639.
(44) Sahoo, B.; Hopkinson, M. N.; Glorius, F. *J. Am. Chem. Soc.* **2013**, *135*, 5505−5508.
(45) Tomioka, H.; Ozaki, Y.; Izawa, Y. *Tetrahedron* **1985**, *41*, 4987−4993.
(46) Frisch, M. J.; Trucks, G. W.; Schlegel, H. B.; Scuseria, G. E.; Robb, M. A.; Cheeseman, J. R.; Scalmani, G.; Barone, V.; Mennucci, B.; Petersson, G. A.; Nakatsuji, H.; Caricato, M.; Li, X.; Hratchian, H. P.; Izmaylov, A. F.; Bloino, J.; Zheng, G.; Sonnenberg, J. L.; Hada, M.; Ehara, M.; Toyota, K.; Fukuda, R.; Hasegawa, J.; Ishida, M.; Nakajima, T.; Honda, Y.; Kitao, O.; Nakai, H.; Vreven, T.; Montgomery, J. A., Jr.; Peralta, J. E.; Ogliaro, F.; Bearpark, M.; Heyd, J. J.; Brothers, E.; Kudin, K. N.; Staroverov, V. N.; Kobayashi, R.; Normand, J.; Raghavachari, K.; Rendell, A.; Burant, J. C.; Iyengar, S. S.; Tomasi, J.; Cossi, M.; Rega, N.; Millam, J. M.; Klene, M.; Knox, J. E.; Cross, J. B.; Bakken, V.; Adamo, C.; Jaramillo, J.; Gomperts, R.; Stratmann, R. E.; Yazyev, O.; Austin, A. J.; Cammi, R.; Pomelli, C.; Ochterski, J. W.; Martin, R. L.; Morokuma, K.; Zakrzewski, V. G.; Voth, G. A.; Salvador, P.; Dannenberg, J. J.; Dapprich, S.; Daniels, A. D.; Farkas, Ö.; Foresman, J. B.; Ortiz, J. V.; Cioslowski, J.; Fox, D. J. *Gaussian 09*, Revision D.01; Gaussian, Inc.: Wallingford CT, 2009.
(47) Barone, V.; Cossi, M. *J. Phys. Chem. A* **1998**, *102*, 1995−2001.
(48) (a) Besler, B. H.; Merz, K. M., Jr.; Kollman, P. A. *J. Comput. Chem.* **1990**, *11*, 431−439. (b) Singh, U. C.; Kollman, P. A. *J. Comput. Chem.* **1984**, *5*, 129−145.

DOI: 10.1021/acs.joc.7b00610
J. Org. Chem. 2017, 82, 6592−6603